Iron inclusion phases of ferromagnetic order within a photonic crystal based on SiO_2

Alexander N. Zakharov,*[a] Alla F. Mayorova,[a] Svetlana N. Mudretsova[a] and Nikolai S. Perov[b]

[a] *Department of Chemistry, M. V. Lomonosov Moscow State University, 119992 Moscow, Russian Federation. Fax +7 495 932 8846; e-mail: alex@zakhar.msk.ru*
[b] *Department of Physics, M. V. Lomonosov Moscow State University, 119992 Moscow, Russian Federation*

DOI: 10.1070/MC2006v016n02ABEH002199

Iron oxide phases of ferromagnetic order obtained by the reductive decomposition of iron(II) oxalate *in situ* synthesised within intraspheric voids of photonic crystals based on SiO_2 were found and studied by TG, DSC and magnetic measurements.

Synthetic noble opals† based on SiO_2 are of growing interest due to their varied applications. The properties of these new materials are of particular importance for functional electronics and laser techniques. Photonic crystals are constituted by nanospheres of amorphous polycondensed SiO_2 and they are typical diamagnetics. However, a system of voids within the opals could be used for the placement of guests of magnetic order. Such nanocomposites may be used as magneto-optic systems for storing and treating information. Here we report the formation of iron oxide phases within intraspheric voids of the photonic crystal based on SiO_2 to yield a material with magneto-optic features.

The noble opals based on SiO_2 are known to contain up to 25% tetrahedral and octahedral voids, which can be filled with a ferromagnetic material. Iron is likely the most important ferromagnetic substance that can be used to modify the photonic crystals.

There are a lot of ways to introduce metal compounds into porous materials. Organometallic complexes were found the most efficient precursors for supporting metals on zeolites[1] due to their high volatility and thermal instability. However, adsorption of these compounds on zeolites is a thermally reversible process. The heat treatment that follows adsorption often results in desorption of the organometallic compound before the decomposition inside the solid yields metal oxide phases. Another drawback of this method is the possibility of the carbonization of metal oxide phases by the decomposition products of the precursor.

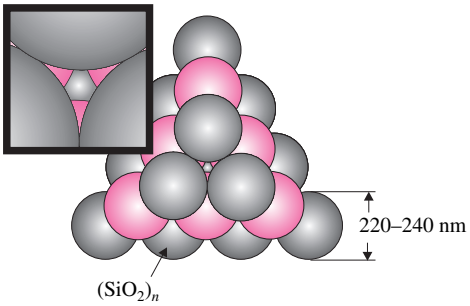

Figure 1 Close-packed cubic structure of a photonic crystal formed with amorphous polymeric SiO_2 nanospheres and a typical octahedral void.

We studied the supporting of iron oxides on the SiO_2 photonic crystals and magnetic properties of the resulting samples. The 'inorganic pathway' was chosen for the supporting of iron oxides instead of the traditional methods using organometallic compounds developed previously.[2]

A close-packed cubic crystal structure of synthetic noble opals is built up of nanospheres of amorphous SiO_2 (Figure 1). The SiO_2 species inside the nanospheres (about 240 nm) form a 3D net resulting from the intermolecular polycondensation. The average dimension of the tetrahedral and octahedral voids within the opal crystal lattice is large (20–40 nm) and can, in principle, be filled with various adsorbate molecules. However, attempts to introduce volatile guest molecules[1,2] within the wide-pore crystal structure of the opal failed, since at the temperature of the experiments desorption was observed before its *in situ* decomposition.

† The samples of the photonic crystals were synthesised by A. V. Guryanov (ZAO 'OPALON', Russia).

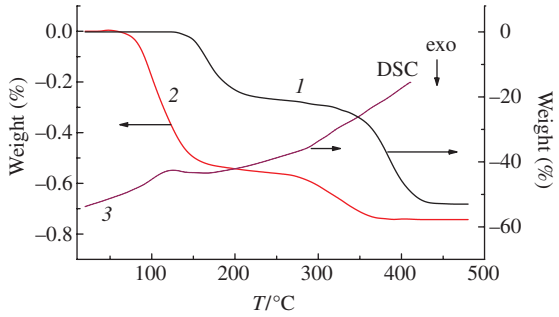

Figure 2 (*1*) TG plot for the pyrolysis of pure $Fe(COO)_2 \cdot 2H_2O$, and (*2*) TG and (*3*) DSC plots for $Fe(COO)_2 \cdot 2H_2O$ supported on the photonic crystals based on SiO_2 (in He); heating rate is 10 K min^{-1}.

On the other hand, inorganic salts are non-volatile and do not migrate over the pores of the photonic crystal. However, these compounds are selectively soluble in organic solvents. This property was used in this work to prepare *in situ* the inorganic precursor – iron(II) oxalate‡ – within the pores of the sample of the photonic crystal.

The formation of $Fe(COO)_2 \cdot 2H_2O$ within the pores of the opal sample impregnated with an aqueous solution of $FeSO_4$ was carried out in ethanol to avoid the reaction of $FeSO_4$ with oxalic acid in solution. Note that $FeSO_4$ is insoluble in ethanol; therefore, the reaction of $FeSO_4$ with $H_2C_2O_4$ undergoes exclusively inside the solid.

The thermal decomposition of the precursor $Fe(COO)_2 \cdot 2H_2O$ within the voids of the photonic crystal was studied by thermogravimetry (TG) and differential scanning calorimetry (DSC).§ Typical plots are presented in Figure 2. The two-stage decomposition of supported $Fe(COO)_2 \cdot 2H_2O$ was observed. These results are in agreement with known data on the decomposition of unsupported $Fe(COO)_2 \cdot 2H_2O$.[3–11] The dehydration of the precursor and the decomposition of $Fe(COO)_2$ (equation 1) occurred simultaneously.[3] The decomposition of $Fe(COO)_2 \cdot 2H_2O$ supported on the photonic crystals was, however, more complex than that of the unsupported material since it was accompanied by the dehydration of the matrix. The heat treatment of the

‡ The photonic crystals calcined at 800 K were treated with a saturated aqueous solution of $FeSO_4$ at room temperature for 30 min. The sample was dried at 333 K for 1 h followed by the addition of an excess of a saturated $H_2C_2O_4$ solution in ethanol. After iron(II) oxalate was formed within the pores, the photonic crystal was extracted with ethanol to remove an excess of the reagents and the soluble products of the reaction. The mixture was heated up to 323 K for 1 h and dried in air at 373 K for 5 h. The impregnation of the photonic crystal with $FeSO_4$ was repeated to reach a maximum loading of the sample.

§ TG and DSC studies were carried out in alumina crucibles in the range 300–720 K under static conditions in He (P_{O_2} = 1 Pa), the heating rate is 10 K min^{-1}, on a Netzsch Simultaneous Thermal Analyzer STA 409.

photonic crystal in helium revealed that the dehydration of the sample took place up to 773 K although water was removed from the sample in the range 315–450 K (Table 1).

$$2Fe(COO)_2 = Fe_2O_3 + 3CO + CO_2 \quad (1)$$

The processes within the pores of the photonic crystal were found to begin at lower temperatures (Table 1). The second step is related with the decomposition of dehydrated iron(II) oxalate. The total weight loss corresponds to the formation of Fe_2O_3 within the pores of the photonic crystal according to reaction (1).

The decrease in the temperatures at which the $Fe(COO)_2{\cdot}2H_2O$ transformations occur in the opal matrix is in agreement with published data[2] for the pyrolysis of adsorbates within narrow-pore supports, such as zeolites of the faujasite type. The thermal instability of adsorbed compounds increases within the pores of the solid.

In order to make sure that no interaction between iron oxide and the support takes place under the experimental conditions, a mechanical mixture was heated up to 773 K. No formation of iron silicate was found in the system. According to the data obtained, no phase transitions occurred in the range 300–773 K. The results in Table 1 evidenced that supported Fe^{II} oxalate undergoes decomposition inside the pores rather than on the external surface of the photonic crystal because the pyrolysis temperatures for $Fe(COO)_2{\cdot}2H_2O$ in the mechanical mixture with the solid are similar to those observed in the decomposition of pure $Fe(COO)_2{\cdot}2H_2O$.

To verify the formation of the iron oxide phases inside the opal matrix, magnetic measurements¶ were carried out under various conditions after the decomposition of $Fe(COO)_2{\cdot}2H_2O$ supported on the photonic crystal. Figure 3 shows the plots of magnetization (*I*) *vs.* magnetic field (*H*) for the obtained samples after subtraction of the magnetic moment of the matrix, which revealed diamagnetic properties, in agreement with the magnetic susceptibility of SiO_2 in quartz. As we can see, the sample prepared by the thermal decomposition of supported Fe^{II} oxalate at 773 K in air exhibited no magnetization (curve *1* in Figure 3). The light-brown colour of the sample indicated the formation of nonferromagnetic Fe_2O_3 in an excess of oxygen:[6]

$$4Fe(COO)_2 + 3O_2 = 2Fe_2O_3 + 8CO_2. \quad (2)$$

The magnetization of this sample appeared after treatment with H_2 at 573 K for 2 h (curve *2* in Figure 2). A magnetic hysteresis loop was observed indicating the reduction of Fe_2O_3 to yield the Fe_3O_4 species with magnetic order. The coercive force and the saturation magnetization (I_s) of this sample were $H_c = 115\pm10$ Oe and $I_s = 0.016$ emu cm^{-3}, respectively.

$$3Fe(COO)_2 + 2H_2 = Fe_3O_4 + 6CO + 2H_2O \quad (3)$$

The thermal decomposition of opal-supported $Fe(COO)_2{\cdot}2H_2O$ at 673 K in H_2 for 2 h resulted in the formation of magnetite inside the pores of the crystal according to reaction (3). The colour of the sample changed by annealing in H_2. This procedure gave rise to the magnetization of the photonic crystal (curve *3* in Figure 3). The coercive force increased up to $H_c = 220\pm30$ Oe. The magnetic behaviour of the reduced sample was found to resemble bulk Fe_3O_4 in the similar thickness range. According to these results, the photon crystal magnetic filling had a magnetic order similar to the ferromagnetic one.

Table 1 Table TG and DSC data obtained under static conditions in helium for pure $Fe(COO)_2{\cdot}2H_2O$ (sample **1**), $Fe(COO)_2{\cdot}2H_2O$ supported on the photonic crystal (sample **2**); photonic crystal (PC), and mechanic mixture of **1** and PC after precalcination up to 450 K; heating rate is 10 K min^{-1}.

Sample	Mass/mg	Temperature/K			
		Decomposition steps		Beginning of thermal effect	
		1st	2nd	1st	2nd
1	14.8	410–460	580–720	410	580
	12.2	410–465	575–715	410	570
2	13.8	350–420	535–665	355	530
	46.7	360–420	535–670	350	535
PC	12.9	315–450	—	310	—
1 + PC	11.8 + 12.9	411–465	610–705	410	625

¶ Magnetic measurements were carried out at room temperature using a vibrating sample magnetometer (accuracy of 8×10^{-11} A m^2).

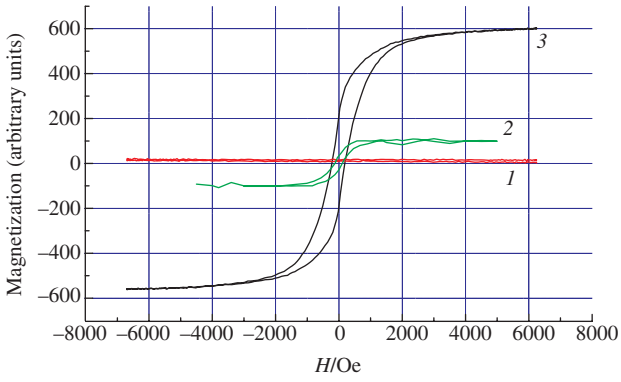

Figure 3 Plots of magnetization *vs.* magnetic field for the photonic crystals modified with the products of thermal decomposition of $Fe(COO)_2{\cdot}2H_2O$ inside the solid under various conditions: (*1*) in air at 773 K, (*2*) in H_2 at 573 K and (*3*) in H_2 at 673 K.

From curves *2* and *3* in Figure 3 the ratio $j = I/I_s$ (I is remaining magnetization) was found equal to 0.23 and 0.36, respectively. Earlier,[12] it was observed that the value of H_c depended on the dimension of Fe_3O_4 particles. The increase in size of the Fe_3O_4 nanoparticles led to a decrease in H_c. However, H_c is a function of not only Fe_3O_4 particle size. The increase in the magnetization saturation after thermal treatment of the iron-supported photonic crystal at an elevated temperature (673 K) in H_2 may be connected with the enhancement of the Fe_3O_4/Fe_2O_3 ratio. Hence, the data obtained here only indicate that magnetically ordered regions within the pores of the photonic crystal are growing by reduction of the sample at 673 K.

According to the loss of the mass of **2** found for the second stage of $Fe(COO)_2{\cdot}2H_2O$ decomposition (Figure 2), which is equal to 0.12±0.03%, the loading of the photonic crystal with iron oxide is 15±4 μmol g^{-1}. This result indicates the partial filling of the octahedral and tetrahedral voids of the sample. On the other hand, the environments offered by the opal void system unambiguously limit the maximum population of the interspherical spacing by the ferromagnetic inclusions. In general, the template synthesis of ferromagnetic inclusions in the restricted environments provides a control over particle size, inter-particle spacing and, probably, particle shape.

References

1 B. V. Romanovskii, *Kinet. Katal.*, 1999, **40**, 742 [*Kinet. Catal.* (*Engl. Transl.*), 1999, **40**, 673].
2 A. N. Zakharov and B. V. Romanovskii, *J. Incl. Phenom.*, 1985, **3**, 389.
3 D. Xue, F. Li, Y. Kong and J. Yang, *J. Phys. Chem. Solids*, 1996, **57**, 461.
4 R. G. Rupard and P. K. Gallagher, *Thermochim. Acta*, 1996, **272**, 11.
5 K. F. Schoch, G. R. Marshall and T. R. Vasilow, *Polym. Mater. Sci. Eng.*, 1995, **73**, 292.
6 H. Kobayashi, T. Ikeda, T. Mitamura, K. Kakizaki and N. Hiratsuka, *Funtai oyobi Funmatsu Yakin*, 1996, **43**, 89.
7 R. Majumdar, P. Sarkar, U. Ray and M. Roy Mukhopadhyay, *Thermochim. Acta*, 1999, **335**, 43.
8 V. Carles, P. Alphonse, P. Tailhades and A. Rousset, *Thermochim. Acta*, 1999, **334**, 107.
9 M. Popa, J. M. Calderon-Moreno, D. Crisan and M. Zaharescu, *J. Thermal Analysis and Calorimetry*, 2000, **62**, 633.
10 E.-H. M. Diefallah, M. A. Gabal, A. A. El-Bellihi and N. A.Eissa, *Thermochim. Acta*, 2001, **376**, 43.
11 V. Baco-Carles, P. Combes, P. Tailhades and A. Rousset, *Powder Metallurgy*, 2002, **45**, 33.
12 F. E. Luborsky and C. R. Morelock, *J. Appl. Phys.*, 1967, **38**, 1005.

Received: 10th June 2005; Com. 05/2530